한국동력기계공학회지 제1권 제1호 pp. 61~69 1997년 12월

◉ 연 구 논 문

Effect of Roughness Position on the Characteristics of Turbulence in Concentric Annuli

S. W. Ahn* and W. J. Lee**

동심환형관에서 난류특성에 미치는 조도위치의 효과

안 수 환*·이 우 재**

Key Words : Turbulence Structure(난류구조), Concentric Annuli(동심환형관), Roughness Element(거칠기 요소), Velocity Gradient(속도구배)

Abstract

본 연구는 동심환형관에서 거칠기가 없이 매끈한 경우, 내측벽에 만, 외측벽에 만, 그리고 양측 모두에 거칠기가 있는 4경우에 대해 직경비가 0.26, 0.39, 그리고 0.56일 때 벽면에 설치된 거칠기위치들이 난류유동장에 미치는 효과를 실험적으로 조사하고자 한다. 최대속도와 전단응력이 0인 지점들, 시간평균속도의 구배들, 그리고 와확산계수들을 X형 열선풍속계와 이중 피토튜브를 사용하여 측정하였다. 본 연구를 통하여 동심환형관에 설치된 거칠기들이 난류유동에 미치는 효과에 대한 정량적자료를 제시할 수 있었다.

1. INTRODUCTION

Our knowledge of the structure of the turbulent fluid flow through channels is based almost exclusively on the experimental results for the turbulent fluid flow through circular tubes and between parallel plates. Such fluid flows are very special cases of channel flows, because these two particular flow channels generate a symmetric velocity profiles, and therefore the positions of the zero shear stress and the maximum velocity coincide. However, the annular channel fluid flows of practical importance in the heat exchanger system generally have more complex boundary conditions. In these non-circular channels, the velocity profiles are asymmetric, and therefore the position of the zero shear stress is not coincident with the position of the maximum velocity.

* 경상대학교 기관공학과, 해양산업연구소
** 경상대학교 정보통신공학과

For this reason, it has attracted the attention of researchers in the hope that its analysis would resolve some of the evident difference between these two basic flow situations, i. e., symmetrical and asymmetrical flows. Accordingly, Brighton[1] for the first time published the experimental results on the turbulence intensities in three directions, and on the radial shear stress in smooth annuli. Brighton assumed that the positions of the zero shear stress and of the maximum velocity coincided, which has been shown to be untrue[2]. Garimella and Christensen[3] have presented the results of a comprehensive study of the pressure drop in concentric annuli with spirally fluted inner tubes for the laminar, transition, and turbulent flow regimes. Ahn et al.[4,5,6,7] have investigated the structure of turbulence in concentric annuli with roughness elements at the three different radius ratios. In the present study, the effects of artificial roughness elements and their positions on the turbulent fluid flow in concentric annuli are presented.

2. EXPERIMENTAL STUDIES

The experimental programme undertaken in the present study is designed to determine the positions of the maximum velocity and zero shear stress, velocity profiles, friction factor, turbulence intensities, and turbulent shear stresses for the turbulent fluid flow in a concentric annulus with artificial roughness elements on walls. Air was chosen as the working fluid. The static pressure measurements were made with a MKS pressure transducer and the calibration of which was made against a micro-manometer (FCO-12) at frequent intervals. Velocities were measured with a X-type hot wire anemometer, and the positions of zero shear stress and maximum velocity were measured with a X-type hot wire anemometer and a double pitot tube. The radius ratios of

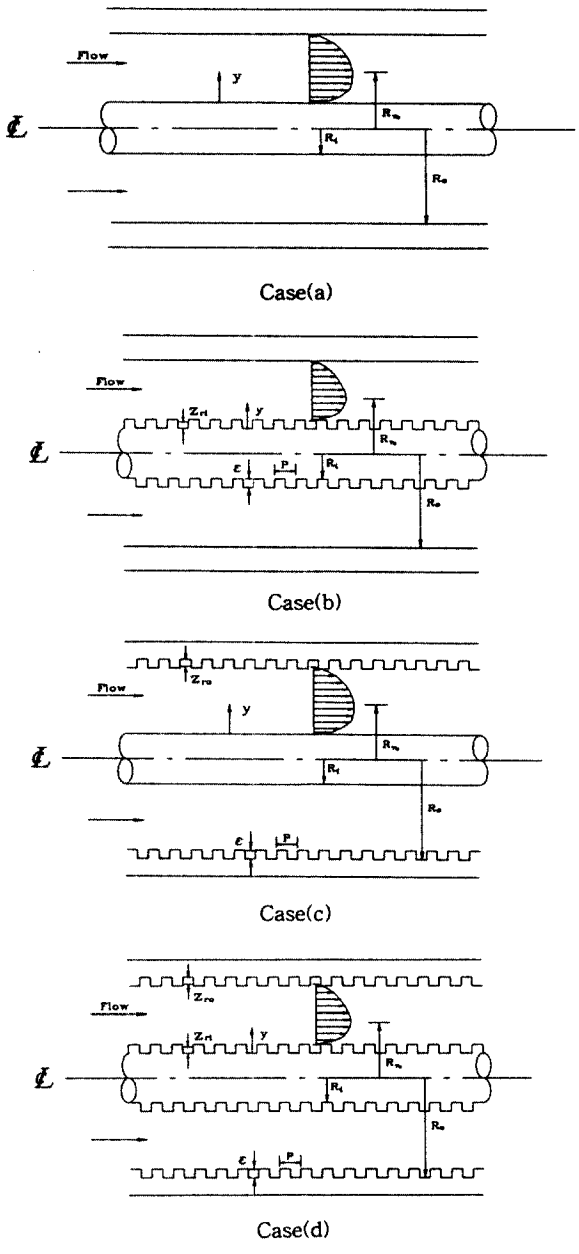

Fig. 1 Idealized model

the test annuli, R_i/R_o, were 0.26, 0.39, and 0.56, respectively. The main apparatus is about 6.1 meter in length. Air is drawn through a flow measuring orifice into an air filter and then through a bell-mouthed contraction section into the test section by a blower (0.8 kW, 3400 RPM) located at the extreme downstream end. The bell-mouthed section (the minimum inner diameter, 97mm; the maximum inner diameter, 160mm) were made from cast iron and the blower fan is rated 9 m^3/min at 520 mm Aq. The essential dimensions of the annular test section are given in Table 1. A specially designed traversing mechanism carries the measuring instrument. With this mechanism, the relative radial displacement of a probe is measured within 0.025 mm by electrical contact. The core tubes were supported at three locations by 3-point carriers which allowed for precise radial adjustments of the core tube. When the test sections were assembled and aligned, the concentricity of the core to the outer tube was checked. The eccentricity due to the lack of straightness of the tubes was negligible in most cases, but the maximum of 2% was noted. The orifice of the flow rate measurement was calibrated by the numerical integration of the velocity profiles measured at the test sections. The range of Reynolds number covered were from 15,000 to 66,000, approximately, at which the characteristic lengths were used with $2R_o$-$2R_i$. The pressure and temperature of the ambient air are also recorded before each run. All the measurements were carried out only late in the night to avoid disturbances on the main power supply. The main experimental variables for the present study are the radius ratio (α) for a fixed roughness pitch to height (P/ε =2) as shown in Fig. 1. Two constant temperature anemometers (C. T. A., TSI Model 1054 A) with an X-type hotwire probe and a universal waveform analyzer (D-6000 Model 611, Data Precision Inc.) were used and the calibration was done with a pitot tube of 4 mm in diameter and 350 mm in length with a digital micro-manometer (Model FCO-12). The outputs from C. T. A. Bridge that are prevented from aliazing by passing through 5 kHz low-pass filter were simultaneously sampled as digital

Table 1 Essential dimensions unit:mm

		O. D.	I. D.	material	α = (Ri/Ro)	De= 2(Ro-Ri)
case(a)	outer tube	113	97	copper	0.26, 0.39, and 0.56, respectively	71.8, 58.4, and 43, respectively
	core tube	25, 38, 54	23, 36, 52	copper		
case(b)	outer tube	113	97	copper		
	core tube	25, 38, 54	22, 35, 51	acryl		
case(c)	outer tube	117	97	Al-alloy		
	core tube	25, 38, 54	23, 36, 52	copper		
case(d)	outer tube	117	97	Al-alloy		
	core tube	25, 38, 54	22, 35, 51	acryl		

values by means of 14-bit A/D converter equiped in the universal waveform analyzer, and then were recorded at the diskettes through Data Recorder.

3. RESULTS AND DISCUSSION

3.1 POSITIONS OF MAXIMUM VELOCITY AND ZERO SHEAR STRESS

The fully developed region could be determined from the pressure gradients along the channel distance and from the mean velocity profiles. The region 1.28 m away from the entrance of the flow channel could be considered as the fully developed one for all the cases of the annuli used in the study.

Figs. 2-5 show the variation of the positions of the maximum velocity and the zero shear stress. All the figures show that the two positions do not coincide. The phenomenon may be attributed to an asymmetrical fluid flow in a concentric annulus. One has not been able to explain the non-coincidence of two positions theoretically. For the measurement of the maximum velocity position, a double pitot tube was used, and a hot wire anemometry system

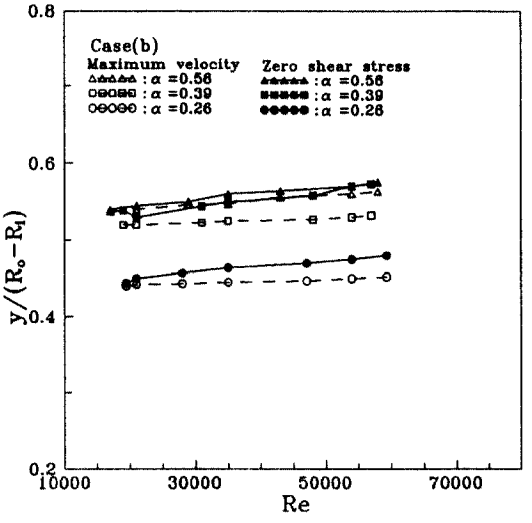

Fig. 3 Maximum velocity positions against zero shear stress positions (Case(b))

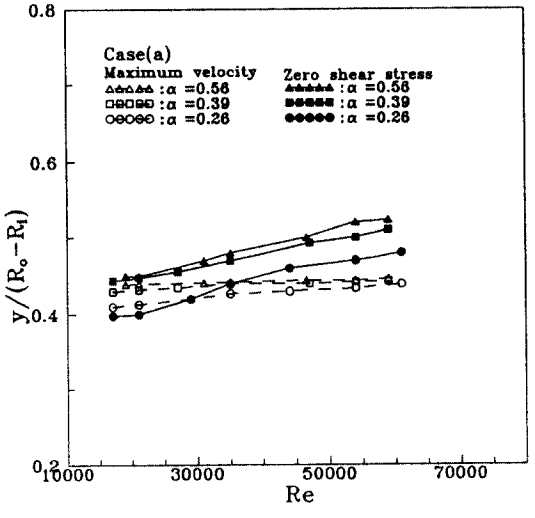

Fig. 2 Maximum velocity positions against zero shear stress positions (Case(a))

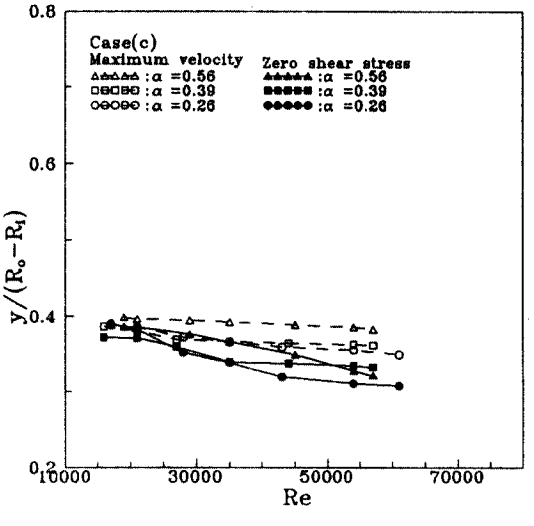

Fig. 4 Maximum velocity positions against zero shear stress positions (Case(c))

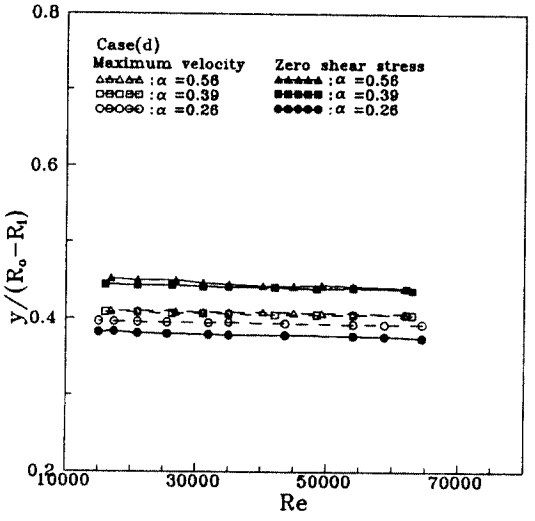

Fig. 5 Maximum velocity positions against zero shear stress positions (Case(d))

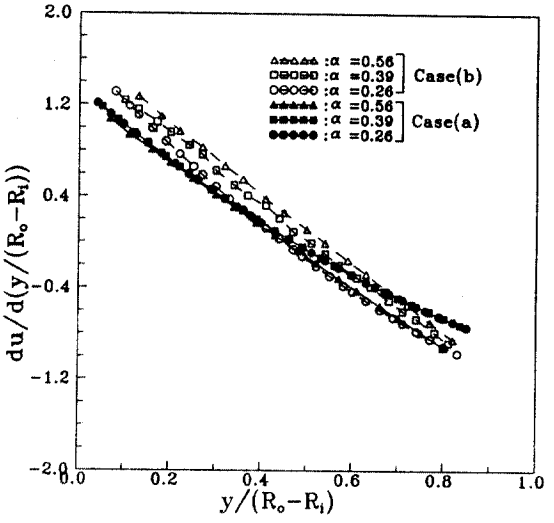

Fig. 6 Velocity gradients at Case (b) at Re=54,000

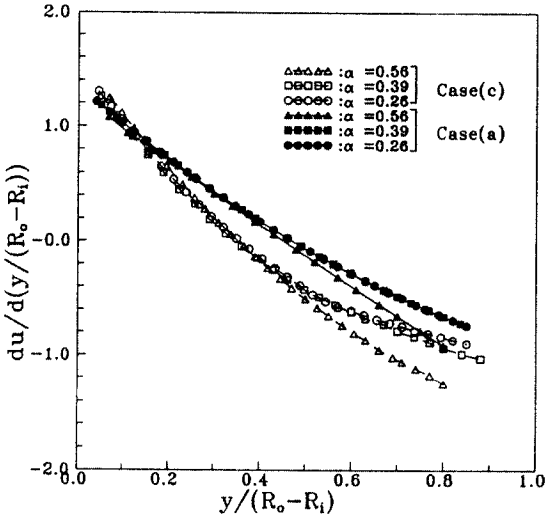

Fig. 7 Velocity gradients at Case (c) at Re=54,000

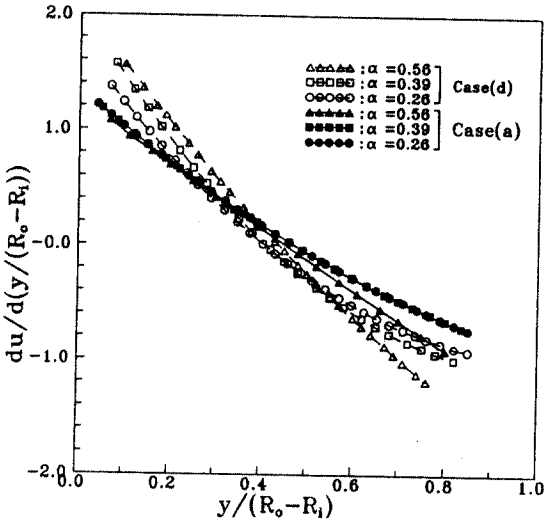

Fig. 8 Velocity gradients at Case (d) at Re=54,000

was used for zero shear stress. For the smooth annulus (Fig. 2), the two positions are located in the region closer to the outer wall at the higher radius ratio. Though the maximum velocity position are almost independent upon Reynolds number, the zero shear stress positions are more strongly influenced by Reynolds number. It is probable that the shear stress distributions are more dependent upon an asymmetrical flow characteristics of the annulus.

For the Case (b) as shown in Fig. 3,

with an increase in the radius ratio, α, both the maximum velocity and zero shear stress points get closer to the smooth outer wall. The variation in accordance with Re indicates stronger diffusion of turbulent eddies from the rough toward the smooth side as the velocity indicates, and the momentum exchange near the rough wall becomes more vigorous. These points deviate more from the center-line of the channel toward the smooth wall with an increase in α (up to α = 0.56) (Fig. 3). This may be expected since a higher α would imply a more vigorous momentum exchange than a lower α. For Case (c), the opposite phenomena are seen as shown in Fig. 4. The positions for Case (d) shown in Fig. 5 are least affected by Reynolds number among the four cases studied. It seems that the eddy diffusivities generated from both the roughened walls move toward the center of the channel.

It is often assumed in theory that, without any justification, the position of the zero shear stress coincides with the radius of the maximum velocity. The experimental results of Kjellström and Hedberg[8] showed that, for partially roughened annuli, there was a small but significant difference between the radius positions of the maximum velocity and the point of the zero shear. In the present study, one also obtained little deviation between the two points as shown in Figs. 2-5.

3.2 VELOCITY GRADIENTS

The velocity gradients are calculated from time-mean velocity profiles through a numerical differentiation method based on the principles of the Largrangian interpolation of polynomials. The measurements for the velocity distributions were made with a X-type hot wire probe. The solid symbols obtained from the smooth annuli of Case (a) are included in Figs. 6-8 as a reference to check the effect of the position of the roughness elements. For Case (a), the values from three different radius ratios at Re=54,000 hardly differ from one another comparing with the others. These phenomena are attributed to the fact that Case (a) has not a rough element on the wall sensitive to the velocity profiles. Among the three cases (b), (c) and (d) in Figs. 6-8, Case (d) has the steepest slope. This fact is that both wall roughness elements in annuli make the velocity profile sharp at same Reynolds number. There is a little deviation between maximum velocity positions in Figs. 2-5 and zero velocity gradient positions in Figs. 6-8. This is attributed to different experimental apparatus; i.e., a double pitot tube and a X-type hot wire anemometer.

3.3 EDDY DIFFUSIVITY FOR MOMENTUM, ε_M

Obtaining static pressure gradients (dp/dx) by averaging the pressure gradients at five axial distance positions in the fully developed region and zero shear stress positions by using X-type hot wire anemometer, and then applying them to momentum conservation equation, the shear stress distributions in the inner and outer zones from zero shear stress positions can be represented as follows:

$$\tau = \frac{dp}{dx}\left(\frac{r^2 - R_m^2}{2}\right)\frac{1}{r} \qquad R_m \le r \le R_o \tag{1}$$

$$\tau = -\frac{dp}{dx}\left(\frac{R_m^2 - r^2}{2}\right)\frac{1}{r} \qquad R_i \le r \le R_m \tag{2}$$

where R_m is the position of zero shear

stress. And the momentum equation in the fully developed turbulent flow of the channel by using eddy diffusivity for momentum, ε_M can be shown as follows:

$$\frac{\tau}{\rho} = \varepsilon_M \frac{du}{dr} \tag{3}$$

The eddy diffusivity for momentum, ε_M from Eq. (3) can be derived as:

$$\frac{\varepsilon_M}{\nu} = \frac{(\tau/\rho)/\nu}{du/dr} \tag{4}$$

Where the eddy diffusivity for momentum, ε_M can be obtained from the velocity gradients and local shear stresses shown in Eqs. (1) and (2). And another method for obtaining the eddy diffusivity for momentum, ε_M is to divide the Reynolds shear stresses measured with X-type anemometer by time-mean velocity gradients as follows:

$$\frac{\varepsilon_M}{\nu} = \overline{u'v'}/(\frac{du}{dr}\nu) \tag{5}$$

The distributions of the eddy diffusivities for momentum, ε_M, for developed turbulent flow in concentric annuli with the surface roughness are shown in Figs. 9-12. The experimental eddy diffusivities for momentum, ε_M, were computed from the mean velocity gradients shown in Figs. 2-4 through the definition of ε_M given by Eqs. (4) and (5), respectively. The velocity gradients were determined from the time-mean velocity distributions by using a numerical differentiation method based on the principles of the Largrangian interpolation of polynomials. The examination of Cases (a), (b), (c) and (d) shown in Figs. 9-12. indicates that the eddy diffusivities increase to a peak on both region of the flow streams and then decrease near the boundary layer edge or near the radii of maximum velocity positions, but does not go to zero. Near the edge of boundary layer, it is extremely difficult to obtain accurate velocity gradients, and therefore, the experimental results in these regions are less reliable. There is an interesting feature that, on the contrary to general opinion, the eddy diffusivities for Case

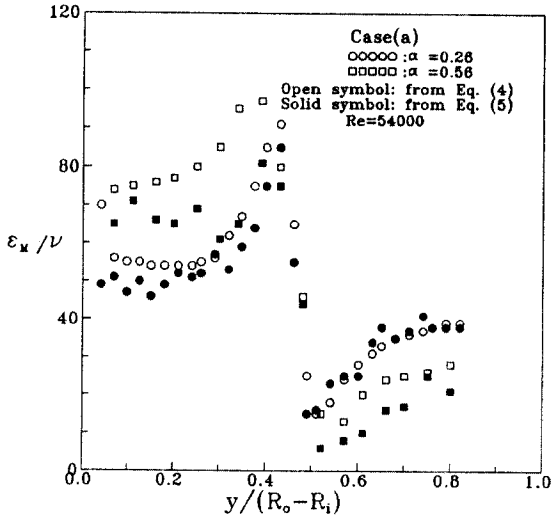

Fig. 9 Eddy diffusivity for momentum for Case (a)

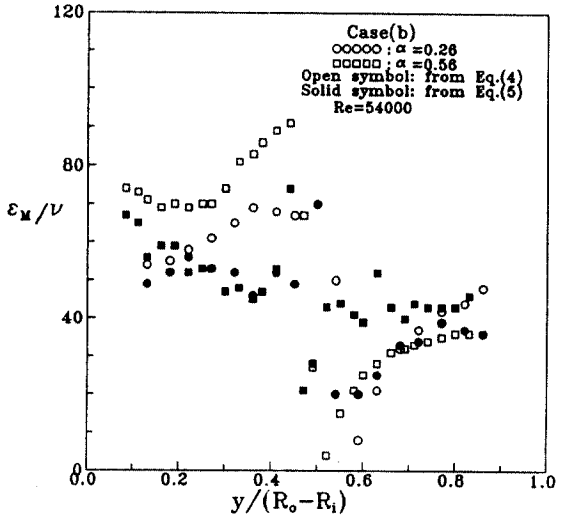

Fig. 10 Eddy diffusivity for momentum for Case (b)

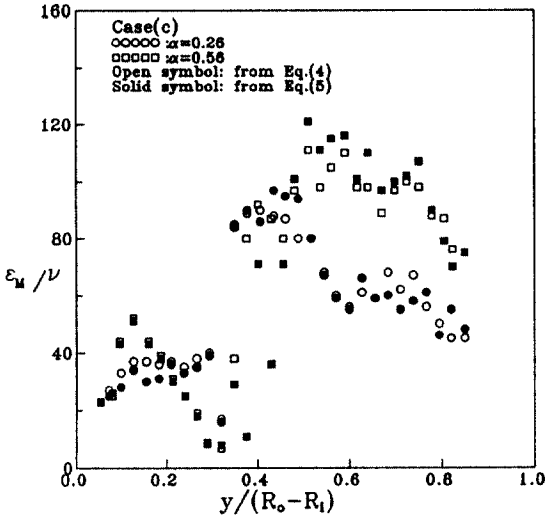

Fig. 11 Eddy diffusivity for momentum for Case (c)

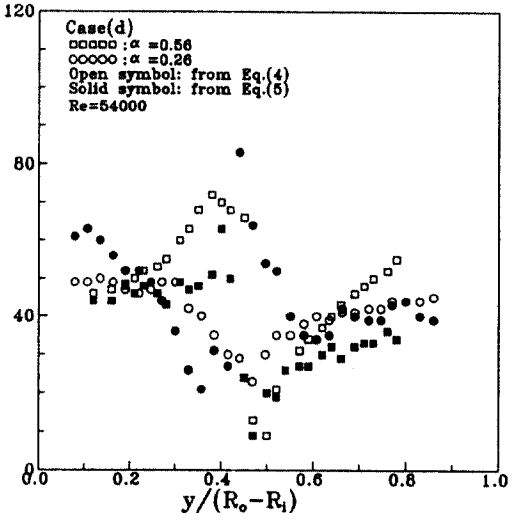

Fig. 12 Eddy diffusivity for momentum for Case (d)

(d) having both rough wall in annuli become lowest. This is because the eddy diffusivities are strongly dependent on the vortex stretching related to turbulent shear stresses as shown in Eqs. (4) and (5).

4. CONCLUSIONS

The following conclusions were derived from the experimental studies made on the turbulence structure characteristics of the fully developed turbulent fluid flow in concentric annuli of the four case studies.

1) In all four cases, the maximum velocity positions are almost independent of Reynolds number, but the positions of zero stress stresses are strongly affected by Reynolds number.
2) Among the three cases of (b), (c) and (d), the velocity gradients of Case (d) have the steepest slope.
3) The eddy diffusivities for Case (d) having both rough walls in annuli become lowest.

ACKNOWLEDGEMENT

The present paper was partially supported by Research Fund from the Institute of Marine Industry in the College of Marine Science of Gyeongsang National University.

REFERENCE

1) J. B. Brighton, "The Structure of Fully Developed Turbulent Flow in Annuli," Ph. D. Thesis, Purdue University, 1963
2) K. Rehme, "Turbulent Flow in Smooth Concentric Annuli with Small Radius Ratios", J. of Fluid Mechanics, Vol. 64, pp.263~287, 1974
3) S. Garimella and R. N. Christensen, "Heat Transfer and Pressure Drop Characteristics of Spirally Fluted Annuli: Part 1 - Hydrodynamics", Trans. ASME, J. of Heat Transfer, Vol. 117, pp. 54~60, 1995
4) S. W. Ahn and K. C. Kim, "Fully Developed Turbulent Flow and heat

Transfer in Rough Annuli", International Communication in Heat and Mass transfer, in press.

5) S. D. Park, "Developing Turbulent Flow in Concentric Annuli: An Analytical and Experimental Studies", Ph. D. Thesis, Dept. of Mech. Eng., University of Ottawa, 1971

6) S. W. Ahn, K. C. Kim and Y. P. Lee, "Fully Developed Turbulent Flow and Heat Transfer in Concentric Annuli with Square-ribbed Roughness", 3rd JSME/KSME Fluids Engineering Conference, Sendai, Japan, pp. 524~529, 1994

7) S. W. Ahn and K. C. Kim, "Turbulent Flow in Annuli depending on the Position of Roughness", J. of KSME(B), Vol. 21, No. 7, pp. 891~889 (in Korean), 1997

8) B. Kjellström and B. Hedberg, "On Shear Stress Distributions for Flow in Smooth or Partially Rough Annuli", AB Atomenergi, Studsvik, Rep. AE-243, 1966